

Patterned Hydrophobic Gas Diffusion Layers for Enhanced Water Management in Polymer Electrolyte Fuel Cells

F. Calili-Cankir ^{a,b*}, E.M. Can ^{c,d*}, D.B. Ingham ^a, K.J. Hughes ^{a*}, L. Ma ^a, M. Pourkashanian ^{a, e}, S.M. Lyth ^{a,c,f,g}, M.S. Ismail ^h

^a Energy 2050, Department of Mechanical Engineering, Faculty of Engineering, University of Sheffield, Sheffield, S3 7RD, United Kingdom

^b Department of Mechanical Engineering, Iskenderun Technical University, Hatay, 31 200, Turkiye

^c Next-Generation Fuel Cell Research Centre (NEXT-FC), Kyushu University, Fukuoka, 819-0395, Japan

^d Department of Mechanical Engineering, Kirsehir, Ahi Evran University, Kirsehir, 40 100, Turkiye

^e Translational Energy Research Centre, University of Sheffield, Sheffield, S9 1ZA, United Kingdom

^f Department of Chemical and Process Engineering, University of Strathclyde, Glasgow, G1 1XL, United Kingdom

^g School of Mechanical and Mining Engineering, University of Queensland, Brisbane, St Lucia, QLD 4072, Australia

^h School of Engineering, University of Hull, Hull, HU6 7RX, United Kingdom

Corresponding authors

Tel: +44 114 215 7244

Email addresses: fcalili1@sheffield.ac.uk, fatmacalili@gmail.com (F. Calili-Cankir); can@kyudai.jp (E.M. Can); k.j.hughes@sheffield.ac.uk (K. J. Hughes)

Abstract

Flooding of the cathode due to water accumulation is one of the biggest limiting factors in the performance of polymer electrolyte fuel cells (PEFCs). This study therefore attempts to solve this issue by fabricating gas diffusion layers (GDLs) with differently patterned hydrophobic regions. The GDLs in three different patterns (triangular, diamond, and inverted-triangular) were prepared by brushing a Polytetrafluoroethylene (PTFE) solution onto commercial carbon papers through a mask and tested in PEFCs. The patterned GDLs results in superior performance in all cases compared to a uniformly PTFE-treated GDL. Notably, the oxygen transport resistance is significantly reduced, indicating that the water accumulation in the cathode is avoided. This is attributed to the patterned hydrophobicity gradient providing distinct pathways for water and oxygen. The GDL with triangular patterning displays the highest peak power density, due to the fact that the untreated less hydrophobic region is in direct contact with the cathode outlet in this case, facilitating the removal of excess liquid water. Overall, the study confirms that the GDLs with patterned hydrophobicity could be used to enhance the performance of commercial PEFC systems by facilitating water management, potentially leading to improved efficiency and durability.

Keywords: Polymer electrolyte fuel cells; Gas diffusion layer; Patterned hydrophobicity; Fuel cell performance; PTFE; Water management

1. Introduction

Polymer electrolyte fuel cells (PEFCs) are clean energy conversion devices which are a key focal point of the newly emerging hydrogen economy [1-3]. This is because they exhibit high efficiency, operate at relatively low temperature, and display rapid start-up [4-6]. Typically PEFCs comprise flow field plates with embedded gas channels, current collectors, gaskets, and a membrane electrode assembly (MEA) [7]. The MEA is at the heart of the PEFC, and consists of the polymer electrolyte membrane, electrocatalyst layers, and gas diffusion layers (GDLs). The porous GDL enables the exchange of reactant gases and product water between flow field channels and the catalyst layers (as well as providing electrical contact). As such, it plays a significant role in both the mass transport of reactant gases and the management of water [8]. The GDL is typically a woven carbon fibre paper containing relatively large pores to facilitate mass transport. However, at high current density, the rate of water generation at the cathode electrocatalyst can block these pores, resulting in a voltage drop due to mass transport limitation of the reactant gases. This is known as flooding and is one of the biggest limiting factors in PEFC performance. Water management in PEFCs is therefore critical, and the GDL is typically treated with a hydrophobic agent to aid the removal of excess water from the cathode.

Polytetrafluoroethylene (PTFE) is a common hydrophobic polymer that is generally used to treat the GDLs. The selected loading of PTFE on the GDL is a trade-off between adding enough material to obtain sufficient hydrophobicity, without compromising the porosity or electrical conductivity. Several groups have investigated the effect of varying the PTFE content on the GDL characteristics. For example, Giorgi et al. [9] reported that GDL porosity decreases as the PTFE content increases, obtaining optimal performance with a PTFE content of a 20 wt.%, and also confirming that flooding really occurs when untreated GDLs are used. Similarly, Velayutham et al. [10] reported an optimum PTFE content of 23 wt.%.

Meanwhile, Park et al. [11] reported that the rate of water removal from the GDL decreases as PTFE loading increases, hence showing that water evaporation and the shear force play a major role in water transport rather than capillary pressure.

We previously showed that the in-plane gas permeability of GDLs decreases as PTFE loading increases [12], whilst a maximum in through-plane permeability is reached at a PTFE loading of 5 wt.% [13]. Also, we showed that the in-plane electrical conductivity is not affected by PTFE content, whereas the through-plane contact resistance increases significantly with PTFE content [14]. Similarly, we showed that the in-plane thermal conductivity slightly increases with increasing PTFE loading (attributed to the reduction in contact resistance), but that the through-plane thermal conductivity significantly decreases with PTFE content, owing to the relatively low thermal conductivity of PTFE [15] [16]. Fishman and Bazylak [17] investigated the impact of PTFE treatment on the distribution of the through-plane local porosity of the GDL. They observed that the PTFE treatment led to a decrease in porosities near the surface regions and PTFE distribution is not uniform throughout the GDL.

Meanwhile, Mortazavi and Tajiri [18] investigated the effect of PTFE content on the dynamic behaviour of water droplets, showing that the droplet detachment diameter decreased for higher PTFE contents, attributed to reduced GDL roughness. Furthermore, in the case of untreated GDLs, droplet detachment was not observed because of the significantly lower contact angle. Alternative hydrophobic polymers to PTFE have also been investigated, including perfluoropolyether (PFPE) [19, 20], fluorinated ethylene propylene (FEP) [21, 22], and polyvinylidene fluoride (PVDF) [23, 24]. Similarly, we have previously investigated the application of superhydrophobic fluorinated carbon materials to enhance water management in GDLs [25, 26].

One proposed method to further enhance water management is to provide separate hydrophobic and hydrophilic regions within the GDL. This is expected to provide separate mass transfer

pathways for oxygen gas and liquid water, thereby reducing the instances of flooding. This has been attempted by several groups, using various different methods. For example, Forner-Cuenca et al. [27] treated GDLs with a hydrophobic FEP solution, applied a patterned mask, subjected the exposed surfaces to an electron beam to generate reactive radical sites, then immersed the GDL in a N-vinylformamide monomer solution to generate patterned hydrophilic sites via radiation grafting polymerisation. This resulted in enhanced PEFC performance due to the mitigation of flooding. In subsequent studies [28-30], the same research group replaced N-vinylformamide with acrylic acid as the hydrophilic monomer, resulting in similarly improved PEFC performance. Similarly, Manzi-Orezzoli et al. [31] used radiation grafting polymerisation to modify a FEP-treated GDL using hydrophilic N-vinylformamide, reporting that this reduced the capillary pressure required to transport water through the channels, lowering the pressure drop within the fuel cell, and ultimately improving performance stability. As such, radiation grafting polymerisation is a promising method to induce patterned hydrophobicity to GDLs, however processing GDLs via radiation grafting is expected to be costly and time-consuming [32].

Meanwhile, Utaka et al. [33] treated GDLs with alternating stripes of PTFE and titanium oxide and observed the formation of water-free oxygen diffusion pathways in the hydrophobic PTFE regions leading to enhanced oxygen diffusivity, whilst liquid water in the hydrophilic titanium oxide regions contributed to hydration of the electrolyte membrane. Similarly, Chun et al. [34] airbrushed mixtures of FEP and carbon black through a shadow mask to create hydrophobic stripes, before shifting the shadow mask across and airbrushing the remaining areas with pure carbon black to create hydrophilic stripes. They reported that increasing the FEP content in the hydrophobic stripes from 10 to 40% resulted in faster water removal from the cathode catalyst layer.

Zhang et al. [35] used a simpler method, whereby they took a conventional PTFE-treated GDL, covered it with a metallic mask, and performed heat-treatment such that the air-exposed regions were rendered more hydrophilic. The mask was designed to match the pattern of the gas flow channels in the flow field. The reported contact angles of the hydrophilic and hydrophobic regions were 75 and 126° , respectively, resulting in improved PEFC performance. The same research group [36] later modified the above method and combined it with ultrasonic spraying to create a hydrophilic-hydrophobic-patterned GDL with stripes of varying pitches of 1, 2 and 3 mm, reporting that a 2 mm pitch increased the peak power density by 30% compared to a conventional GDL.

Chen et al. [37] obtained point-, line-, and flowerlike patterns on the surface of MPLs by recrystallization and pyrolysis of ammonium chloride with different contents in order to improve the removal of excess water and the diffusion of reactant gases. They found that a porosity-graded MPL with a flowerlike pattern showed the best performance, and this is due to the fact that the graded porosity facilitates the water removal from the catalyst layer while the flowerlike pattern accelerates the diffusion of the reactant gases between the catalyst layer and the MPL.

Yu et al. [38] applied a three-dimensional lattice Boltzmann model to investigate the dynamics of liquid water flowing through three GDLs with different PTFE distribution: GDL uniformly treated with PTFE, GDL with half PTFE treatment in the through-plane direction, and GDL with half PTFE treatment in the in-plane direction (sandwich-like PTFE-treated). They showed that the PTFE-treated regions in the non-homogenous configurations drive the liquid water, whereas the untreated regions are completely flooded with water. In a later work, the same research group [39] investigated the effect of the inhomogeneous PTFE distribution in the through-plane direction of the GDL on the two-phase transport using the lattice Boltzmann method. Their findings revealed that the PTFE covering the superficial fibres in the non-

uniform configuration increases the water contact angle and subsequently improves liquid water removal.

Finally, Koresawa and Utaka [40] used vacuum suction of PTFE dispersion through a patterned mask to fabricate GDLs with the dotted and striped hydrophobic regions, reporting oxygen diffusivity three times higher compared to uniformly-treated GDLs. Importantly, they found that the oxygen diffusivity did not depend upon the pattern, but on the overall area of the hydrophobic region through which the liquid water is mostly expelled.

In this study, considering the above works, we propose a single method to create patterned hydrophobicity on GDLs. First, we propose a single treating step through a patterned mask onto a heated stage, to take advantage of the intrinsically less hydrophobic nature of carbon paper compared to PTFE-treated region (rather than treating with two different materials or performing complex electron irradiation or vacuum suction steps). Further, we determine the optimal PTFE loading, and then investigate three different configurations of patterned hydrophobicity: (i) diamond-like, (ii) triangular, and (iii) inverted-triangular configurations. The choice of these patterns is motivated by their simplicity, offering ease of application and potential for practical implementation in the fuel cell industry. The water contact angle, electron conductivity and microstructure of the GDLs are characterised, then they are tested in PEFCs and the oxygen transport resistance is measured.

2. Experimental methods

2.1. Preparation of GDLs

Commercially available and untreated Toray GDLs with 1 cm² (TGP-H-060 Toray Paper, 190 μm) were first washed in ethanol (99.5 vol. %, Wako, Japan) to remove possible impurities from the surface and pores. They were then dipped into a solution of 2.5 wt. % PTFE (diluted

from 60 wt. % PTFE dispersion Teflon™ 30B from Polysciences, Inc) for 1 s then removed and dried to create uniformly PTFE-treated GDLs that were used as reference sample.

Meanwhile, patterned GDLs were fabricated by placing untreated Toray-GDLs on a hot stage at 90 °C and clamping a machined stainless-steel mask over them. The unmasked areas were then carefully brushed with 2.5 wt. % PTFE solution, whilst the high temperature facilitated rapid evaporation of the solvent, preventing bleeding into the masked areas. Finally, all treated GDLs were sintered for one hour at 380 °C in air to melt the PTFE before being cooled to room temperature. It is important to note that the weight of the GDL samples was systematically measured both before and after PTFE treatment, as well as after sintering the samples, to confirm the achievement of PTFE loading within the specific range of 6 and 8 wt. %.

2.2. Water contact angle measurements

The surface water contact angles (WCAs) of the fabricated GDLs were measured adopting the pendant drop method and using a contact angle goniometer (Goniometer FTÅ 200, UK) equipped with a high-resolution camera. A small volume of water (1-2 µl) was dispensed onto the surface of the sample to minimise the effect of gravity. WCAs were obtained from acquired images manually using a protractor as the native software was not able to accurately capture the borders of the droplets and the surface of the GDL. WCAs were measured for both the right- and left-hand sides of the droplet, and repeated for at least 5 droplets on each sample. The data was then averaged and the 95% confidence interval was calculated.

2.3. In-plane electrical conductivity measurement

The GDL specimens were prepared for conductivity tests by cutting them using a scalpel into rectangular-shaped samples with 2.5 cm width and 7 cm length. Five samples, two of which were obtained by cutting the sheet in a direction perpendicular to that of the first three samples,

were prepared by cutting from the same GDL sheet. The in-plane electrical conductivity measurements of the GDL samples were conducted using the four-probe method [41, 42]. A constant current was applied through the “external” two electrodes and the resistance, R (Ω) was computed by dividing the voltage measured by the “internal” two electrodes by the above current. Then, the electrical resistivity, ρ was calculated using the following formula [41]:

$$\rho = CtR \quad (1)$$

where t is the thickness of the GDL (i.e., 190 μm) and C is the correction factor determined by the dimensions of the GDL sample and spacing between the probes [41]. In this study, the resulting correction factor is 0.9973. The electrical conductivity, σ (S/m), was obtained as follows:

$$\sigma = 1/\rho \quad (2)$$

2.4. Surface morphology

The surface morphology of GDL samples was evaluated using scanning electron microscopy (JSM-6010LA, Jeol, UK). The GDL sample was mounted onto an SEM stub using a double-sided carbon tape. The SEM instrument was operated at an acceleration voltage of 20 kV. Other imaging parameters, such as working distance and magnification, were adjusted as needed for optimal image quality and resolution.

2.5. Cell assembly

Pt/C particles (TEC10E, 46.8 wt_{pt} %, Tanaka, Japan) were mixed with 5 wt. % Nafion solution (Wako, Japan), deionized water, and super-dehydrated ethanol (99.5 vol. %, Wako, Japan) to prepare a catalyst ink solution for MEA preparation. The catalyst ink was sonicated in an ultrasonic homogenizer (UH-600, SMT Corporation) for 30 min immediately before spraying

it onto the membrane. The ink was then sprayed using an automated spraying machine (Nordson K.K, C3J) onto both sides of a Nafion 212 membrane placed onto a heated plate (60 °C) and masked to obtain a 1 cm² active area with 0.3 mg Pt loading and a Nafion content of 28 wt. %. The sprayed membrane was then hot-pressed at 132 °C and 0.3 MPa for 3 min (Sinto Digital Press CYPT-10, Japan). The resulting catalyst-coated membrane was sandwiched between two GDLs and placed into a Japanese Automotive Research Institute (JARI) cell with serpentine-type flow fields to form a fuel cell assembly. 5 wt. % PTFE 190 µm Toray-GDL (TGP-H-060 Toray Paper) was used at the anode.

2.6. Single cell polarisation measurement

Fuel cell performance tests were carried out in a fuel cell test station (AUTOPEM-CVZ01, Toyo Corporation, Japan) connected to an electrochemical interface impedance analyser (Solartron SI-1287, Japan) and a frequency analyser (SI-1222B, Japan). Polarisation curves of the fuel cell with uniformly PTFE-treated GDLs (i.e., the reference case) and with different patterned hydrophobic GDLs at the cathode were obtained at a cell temperature of 80 °C and 100% relative humidity. The constant flow rates in counter-flow conditions were 0.139 L/min for the humidified hydrogen stream and 0.332 L/min for the humidified oxygen stream. Each test was conditioned by operating the fuel cell at 0.6 V for three hours before measuring the polarisation curves. The cell resistance was obtained from the impedance spectroscopy at 0.05, 0.1, and 0.2 A direct current loading and subsequently averaged.

2.7. Oxygen transport resistance

The flow rate of reactant gases was set to 1 L/min for both sides of the fuel cell to measure the oxygen transport resistance. The oxygen concentration was set at 2 vol. % and balanced with nitrogen at the cathode side. The limiting current density was measured at 80, 85, 90, 95, and

100% relative humidity at 80 °C cell temperatures for each GDL sample. The total oxygen transport resistance was calculated as follows [25]:

$$R_t = \frac{4FP_{O_2}}{I_{lim}RT} \quad (3)$$

where R_t is the total oxygen transport resistance of the fuel cell (s/m). P_{O_2} is the partial pressure of oxygen (Pa), I_{lim} is the limiting current density at 0.2 V and T is the temperature of the fuel cell (K). F and R are the Faraday's constant (96485 C/mol) and the universal gas constant (8314 J/(mol.K)), respectively.

3. Results and discussion

3.1. GDL characterisation

Commercially available GDLs with varying PTFE loadings were first characterised to gain insights into the optimal amount of PTFE that should be used for the GDLs with the patterned hydrophobicity. The aim is to find the lowest acceptable PTFE loading that can be used to induce hydrophobicity, without compromising the porosity or conductivity of the GDL. The contact angle for the untreated GDL ((i.e., 0% PTFE content) is $128^\circ \pm 3$ and this significantly increases to $150^\circ \pm 2$ for 5 wt. % PTFE loading (Fig. 1). No further increase in contact angle is observed for higher PTFE loadings. Similar studies conducted by Benziger et al. [43], Fairweather et al. [44], Mortazavi and Tajiri [18] and Ismail et al. [45] all report similar results. As such, it is clear that 5 wt. % PTFE is sufficient to result in reasonable GDL hydrophobicity. Another defining aspect of the wettability of the GDL is the water breakthrough pressure. This refers to the pressure at which liquid water permeates through the porous GDL. Mortazavi and Taraji [46] conducted an experiment to determine the water breakthrough pressure of TPG-H-060 Toray carbon papers with varying PTFE loading. They found that treating the surface of the GDL with a certain amount of PTFE (i.e., 10 wt. %) increases the water breakthrough

pressure. However, increasing the PTFE loading beyond that has almost negligible effect on the water breakthrough pressure. Their findings are consistent with our results that highlight the impact of PTFE loading on the contact angle of the GDL (Fig. 1).

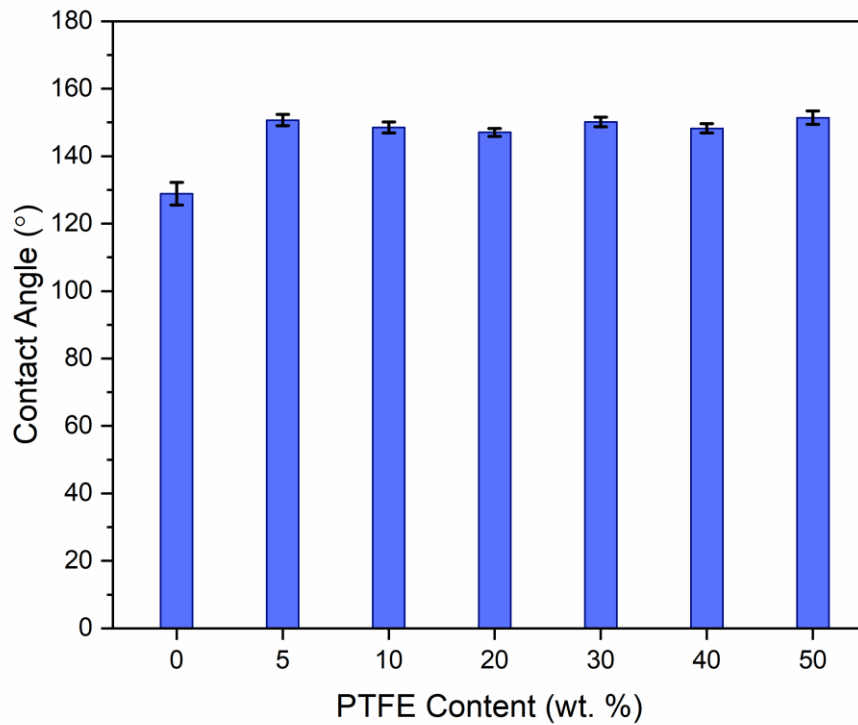


Fig. 1 Water contact angle of uniformly treated GDLs as a function of PTFE content.

The electrical resistivity of three samples for each GDL was then measured to calculate the in-plane electrical conductivity in two different perpendicular in-plane directions. Fig. 2 depicts the values of the in-plane electrical conductivity of the GDL as a function of PTFE content in the two perpendicular principal directions that were arbitrarily designed as 0° and 90° . Since PTFE is an electrically insulating material, one expects that the electrical conductivity of the GDL would decrease as the PTFE loading increases. However, the experimental results indicate that there is no particular trend in electrical conductivity with increasing PTFE. This could be attributed to the fact that the PTFE particles tend to discontinuously stick to the carbon fibres [14], such that the conductive pathways remain largely unaffected. Further, it was

observed that the conductivity is the same in both orientations, attributed to the random orientation of the carbon fibres, leading to lateral isotropy (i.e., that the physical characteristics are uniform in all in-plane orientations).

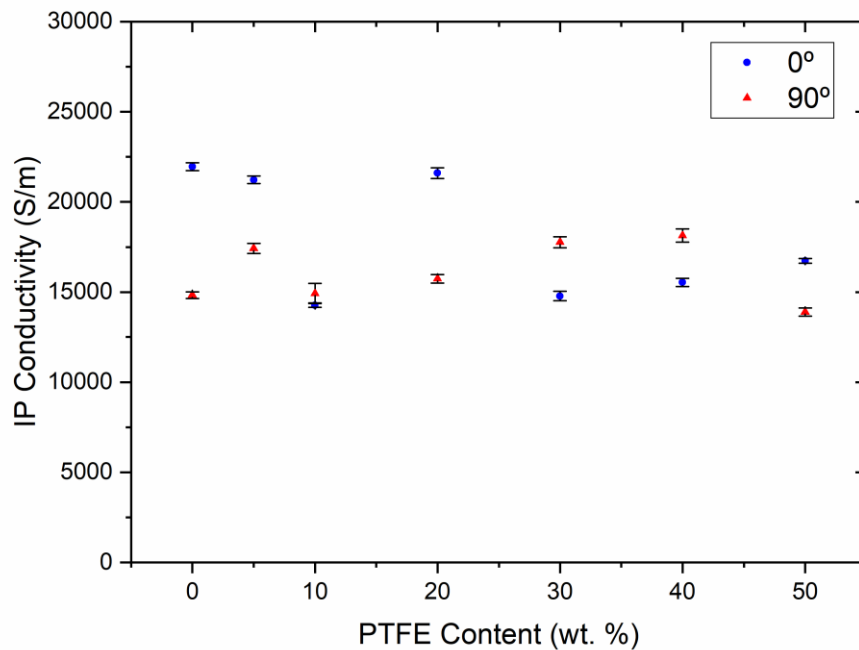


Fig. 2 The in-plane electrical conductivity of uniformly treated GDLs as a function of PTFE content measured in two perpendicular orientations (0° and 90°).

Micrographs of the GDLs confirm the isotropic orientation of the individual carbon fibres (Fig. 3). Furthermore, they reveal some degree of webbing, especially at the apexes between the individual carbon fibres (Fig. 3). The degree of this webbing appears to increase as the PTFE loading increases as expected, and likely result in decreased GDL porosity [18].

To avoid any decrease in porosity which may be detrimental to GDL performance, and since the contact angle and the electrical conductivity are not dependant on PTFE loading (Fig. 1 and Fig. 2), relatively low PTFE loading (6-8%) was applied to untreated Toray carbon papers to create GDLs with patterned hydrophobicity. This has the added advantage of reducing the amount of required PTFE in the GDL, leading to reduced system costs.

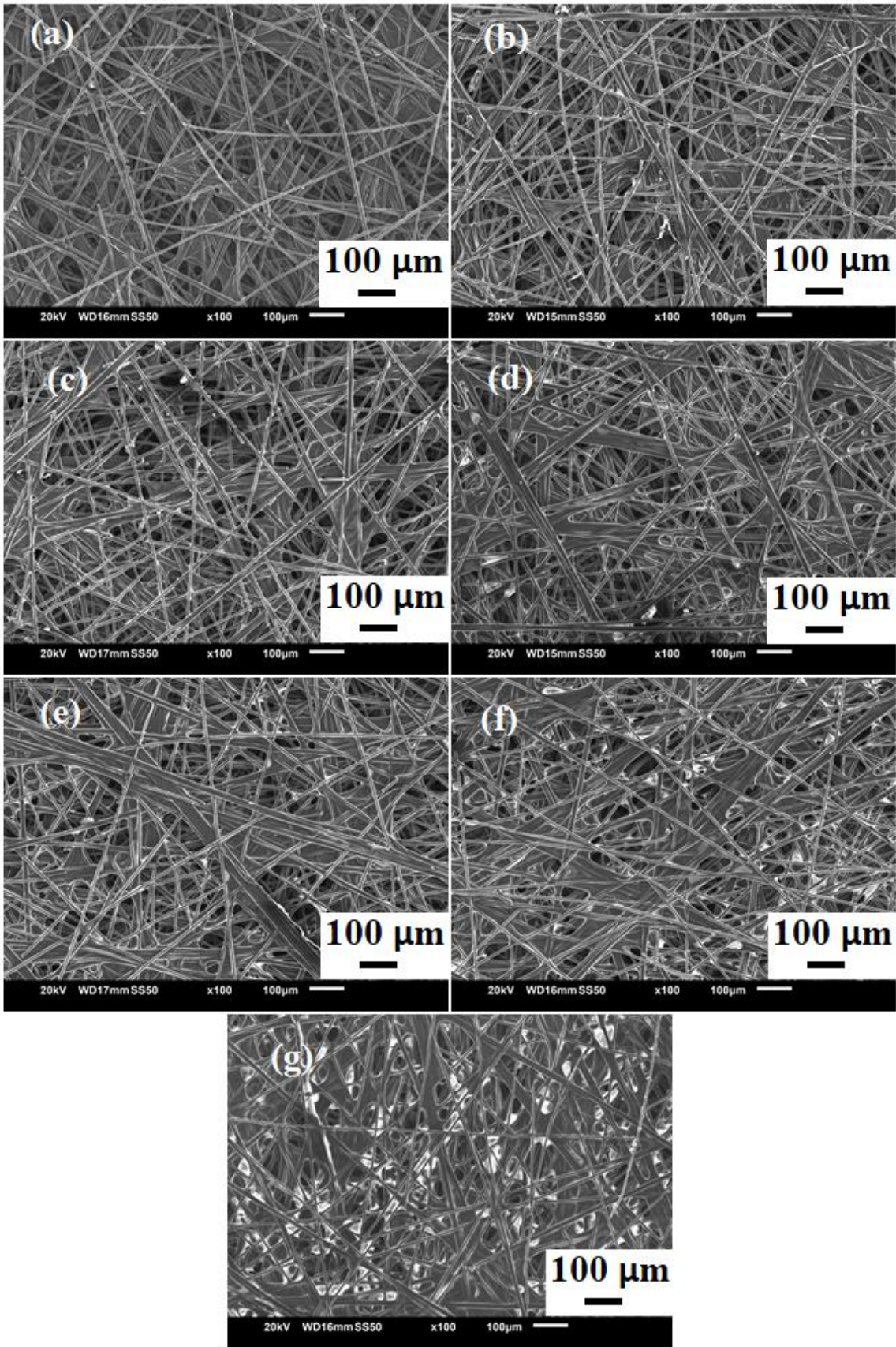


Fig. 3 SEM images of uniformly treated GDLs with (a) 0%, (b) 5%, (c) 10%, (d) 20%, (e) 30%, (f) 40% and (g) 50% PTFE loading.

Patterned GDLs with four different geometries were prepared for electrochemical tests: (i) a uniformly treated reference GDL (Fig. 4a); (ii) diamond-like geometry (Fig. 4b); (iii) triangular geometry (Fig. 4c); and (iv) inverted-triangular geometry (Fig. 4d). A noticeable contrast is observed in photos of the GDLs between the PTFE-treated regions (darker) and untreated regions (lighter). For comparative purposes, a consistent 1:1 ratio between PTFE-treated and untreated regions was maintained in all the patterned GDLs.

Meanwhile, the cathode side endplate of the fuel cell is displayed in Fig. 4e, showing the locations of the oxygen inlet and outlet. It should be noted that the flow channels are fully covered by the GDL samples and in the case of the triangular patterned GDL, the untreated region of the GDL is in direct contact with the cathode outlet, whilst the PTFE-treated region is in direct contact with the cathode outlet in the case of the inverted-triangular pattern (Fig. 4f).

Fig. 5 shows SEM micrographs of the treated and untreated regions of the triangular patterned GDL. In contrast to the photographs in Fig. 4c, the PTFE-treated regions are brighter than the untreated regions in this case. This is because the PTFE-treated regions include fluorine atoms which have a higher atomic number than carbon (9 versus 6), thus tending to generate more backscattered electrons when subjected to SEM electron beams, resulting in a brighter appearance compared to untreated regions [47].

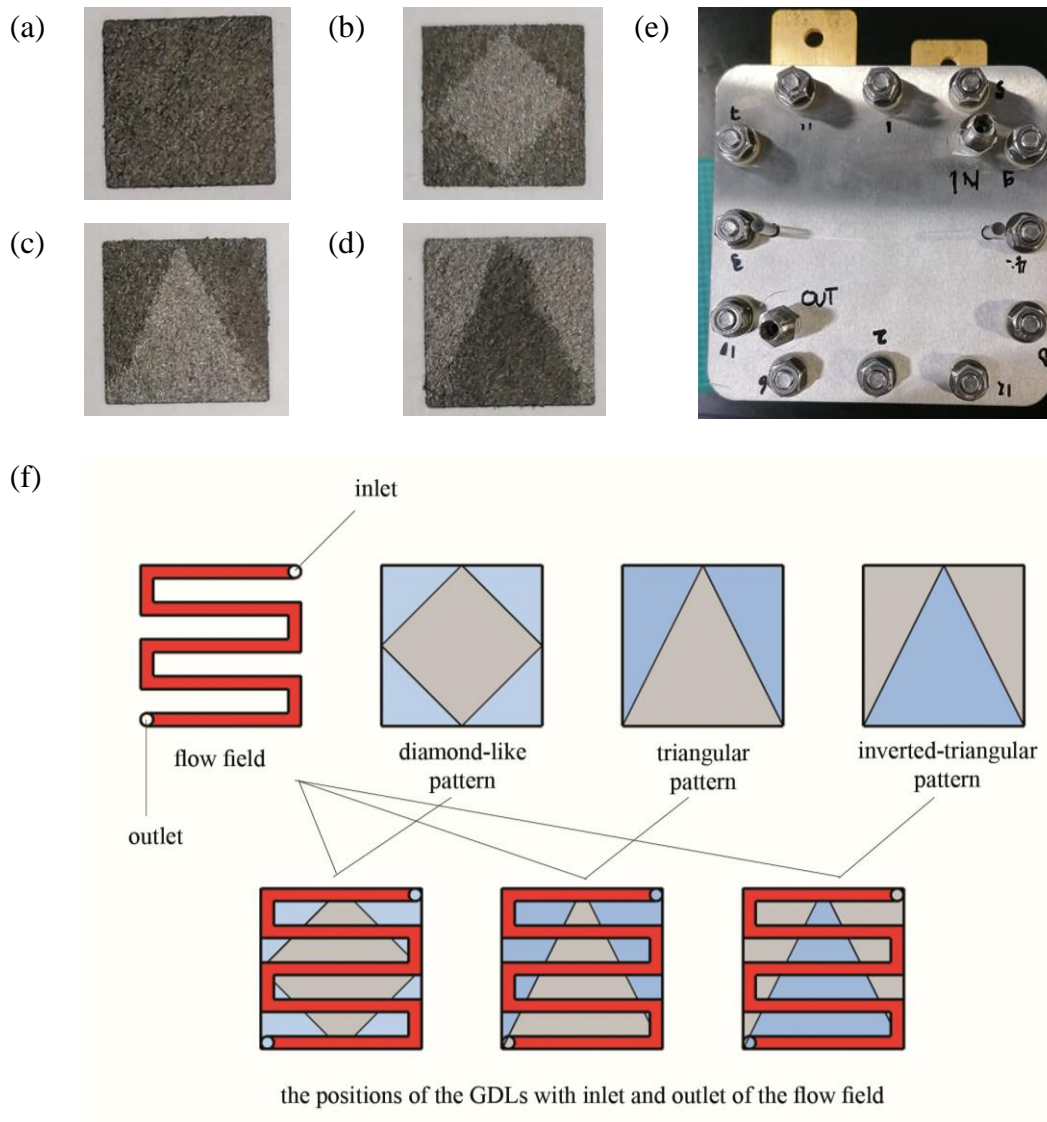


Fig. 4 Photographs of the patterned GDLs: (a) uniformly treated; (b) diamond-like pattern; (c) triangular pattern; (d) inverted-triangular pattern and (e) the cathode side of the fuel cell. (f) The sketch of the cathode flow-field plate showing the position of the GDLs. In the schematic view, blue regions in the GDLs represent PTFE-treated areas while grey regions depict untreated areas.

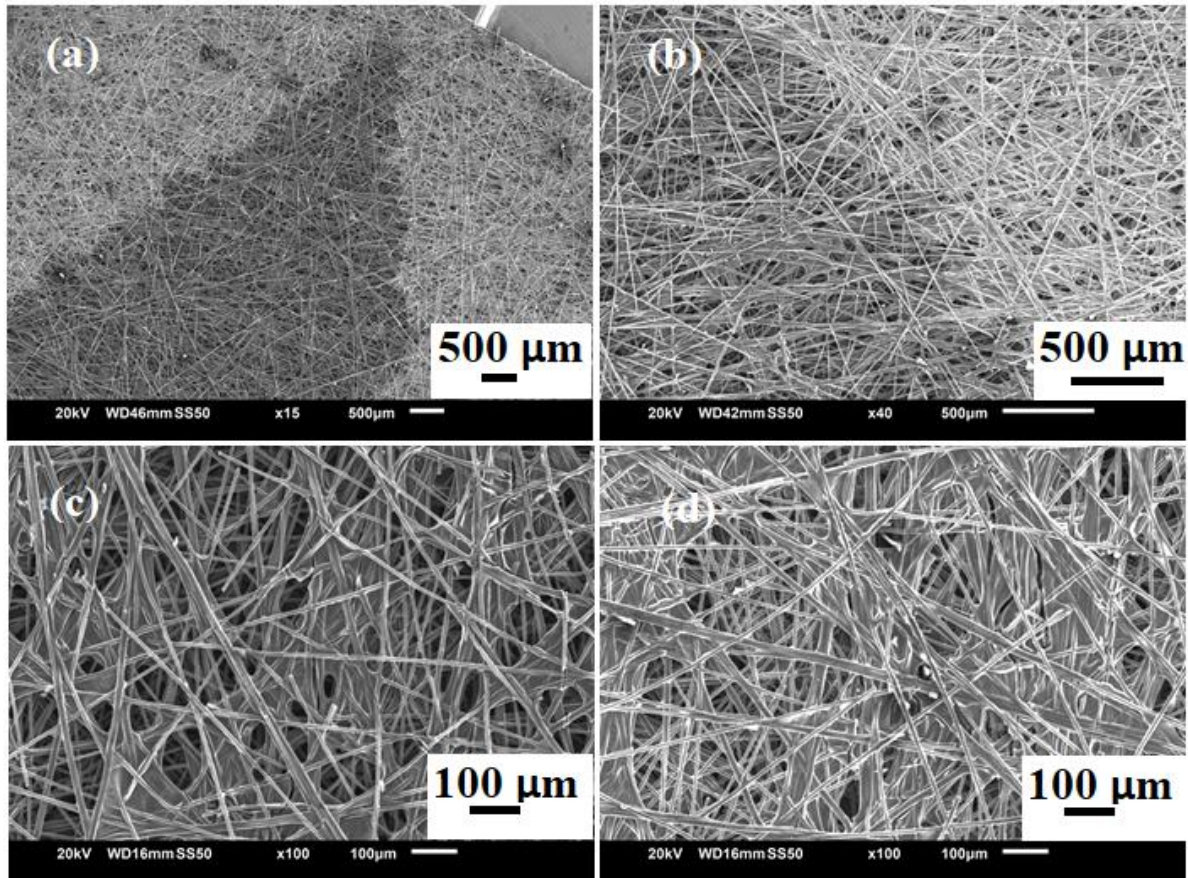


Fig. 5 SEM micrographs of the triangular patterned GDL showing: (a) the apex of the triangle pattern; (b) the interface between the treated (right) and the untreated regions (left); (c) a higher magnification image of the untreated region; and (d) a higher magnification image of the PTFE-treated region.

Fig. 6 shows images of water droplets residing on the surfaces of the various GDLs. The contact angle of the untreated GDL (127° , Fig. 6a) and the uniformly PTFE-treated GDL (149° , Fig. 6b) correspond closely with those of untreated (125° , Fig. 6c) and PTFE-treated (148° , Fig. 6d) regions of a patterned GDL. This confirms that distinct regions of differing hydrophobicity can be created within the GDL using the simple methods employed here. Meanwhile, it is of note that the water droplets tended to readily migrate from higher hydrophobic PTFE-treated regions along the hydrophobicity gradient towards the relatively less hydrophobic untreated regions during the measurement. This provides some initial indication that these patterned GDLs could

be able to enhance mass transport under fuel cell operation by preferentially directing liquid water towards the less hydrophobic regions.

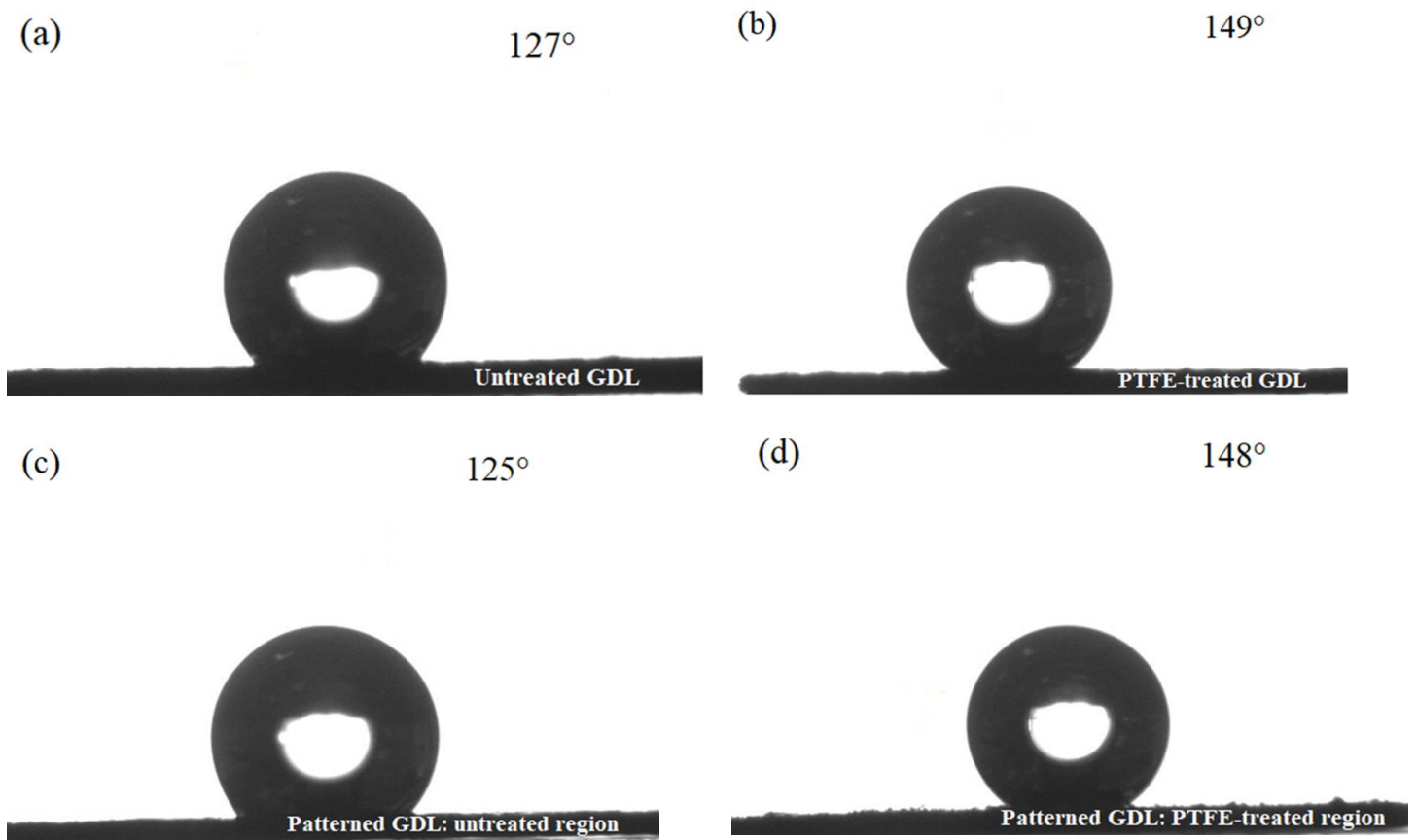


Fig. 6 Images of water droplets residing on the surfaces of GDLs along with the measured water contact angles for: (a) an untreated GDL; (b) a uniformly treated GDL; (c) the PTFE-treated region of a patterned GDL; and (d) the untreated region of a patterned GDL.

3.2. Fuel cell performance

Fig. 7 shows the IR-free cell voltage and the power density as a function of current density for a fuel cell operating with the GDLs, investigated at a cell temperature of 80 °C and under fully humidified conditions. These polarisation curves demonstrate a noticeable enhancement when using the patterned GDLs compared to the uniformly PTFE-treated GDL. The improvement is more profound in the high current density region where the fuel cell is mass transport resistance limited and more susceptible to water flooding. The corresponding limiting current densities

were measured to be 1.23, 1.35, 1.48, and 1.24 A/cm² for uniformly PTFE-treated, diamond-like patterned, triangular patterned, and inverted-triangular patterned GDLs, respectively. The power density curves follow the same trend, with maximum values of 0.54, 0.60, 0.64 and 0.57 mW/cm², respectively.

Meanwhile, Fig. 8 shows the oxygen transport resistance for the investigated GDLs. In all cases, the GDLs with patterned wettability exhibit significantly lower oxygen transport resistance than the uniformly PTFE-treated GDL, across a wide range of relative humidity. Furthermore, the GDL with a triangular wettability pattern exhibits the lowest oxygen transport resistance. This favourable outcome can be attributed to the unique arrangement of triangular pattern, which enhances oxygen diffusion pathways and minimises water accumulation within the GDL. This design facilitates efficient oxygen transport to the cathode catalyst layer, mitigating mass transport losses and contributing to superior fuel cell performance. On the other hand, the GDL with an inverted-triangular pattern displays the highest oxygen transport resistance amongst the patterned GDLs; this is directly linked to increased mass transport losses, particularly at high current densities, due to the reduced capability of this patterned GDL to adequately remove excess liquid. Elevated oxygen transport resistance signifies constrained oxygen flow to the cathode catalyst layer, resulting in a reduction of reaction rate and, consequently, an inferior fuel cell performance.

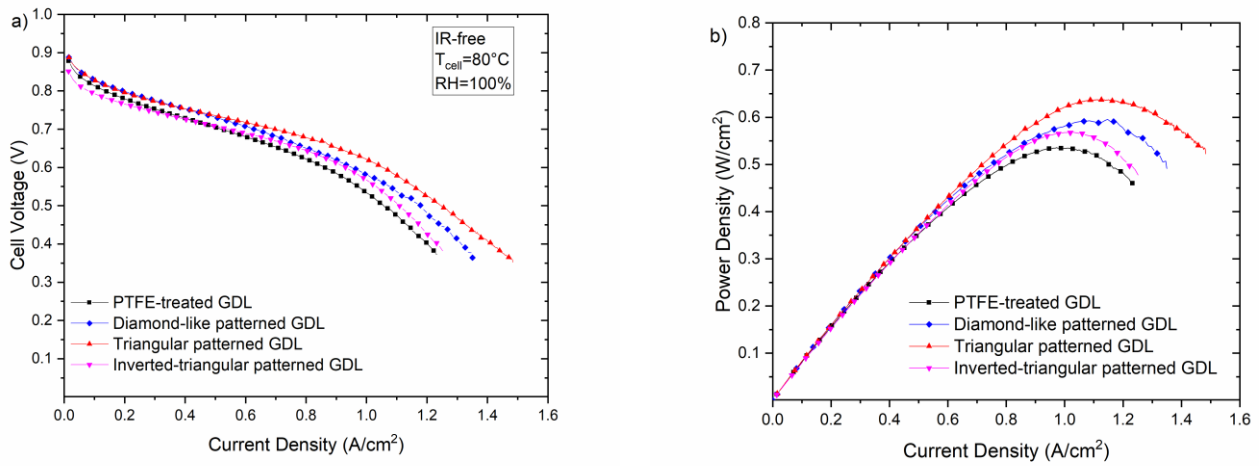


Fig. 7 (a) IR-free cell voltage and (b) power density as a function of current density at cell temperature of 80 °C and 100% RH for uniformly PTFE-treated, diamond-like patterned, triangular patterned and inverted-triangular patterned GDLs.

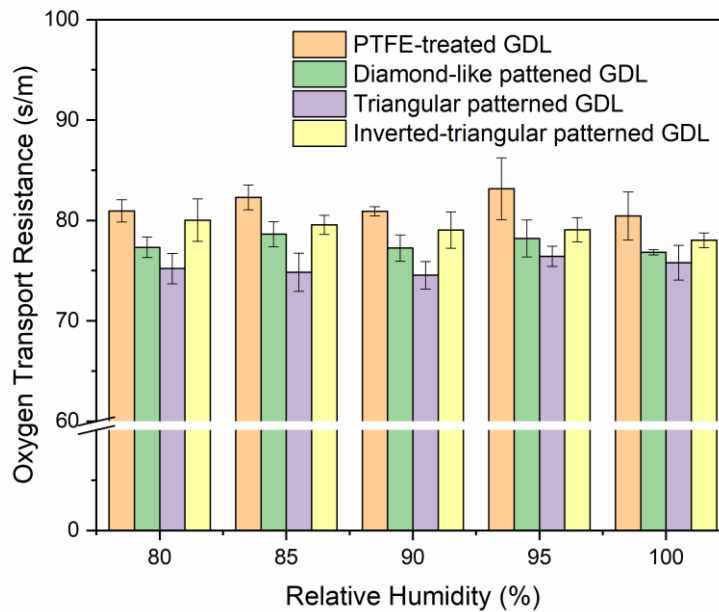


Fig. 8 Oxygen transport resistances for uniformly PTFE-treated, diamond-like patterned, triangular patterned and inverted-triangular patterned GDLs, measured at different values for relative humidity.

These findings confirm that employing GDLs with patterned hydrophobicity can improve oxygen transport to the catalyst layer and therefore lowering mass transport losses. Namely, the water produced at the cathode catalyst layer mainly transport to the untreated regions of the

patterned hydrophobic GDLs, establishing continuous pathways for water removal from the cathode catalyst layer to the flow channels. This leaves the higher hydrophobic regions available to facilitate oxygen transport through the GDL to the catalyst layer, unhampered by flooding at high current density.

Meanwhile, the difference in performance between the triangular and inverted-triangular patterning can be attributed to the position of the cathode outlet. Specifically, the triangular configuration allows for the direct contact between relatively less hydrophobic untreated region of the GDL and the cathode outlet. This arrangement facilitates water removal in the in-plane direction as the hydrophobicity gradient drives water from the more hydrophobic PTFE-treated regions to the relatively less hydrophobic untreated region. The latter region is in direct contact with the cathode outlet where water removal is driven by water concentration difference in the through-plane direction, thus ultimately resulting in the lowest oxygen transport resistance amongst the three patterned GDLs. As such, the positioning of the fuel cell outlet relative to the patterned regions on the GDL should be carefully considered.

This investigation primarily focused on fixed orientations of the patterned GDLs. However, in follow-up studies, it will be of great interest in to investigate the impact of the rotation of the triangular and inverted-triangular patterned GDL samples (and subsequently the impact of the relative position between the treated/untreated regions of the GDL and the cathode outlet) on the fuel cell performance.

Notably, MPL coating has not been applied to the patterned hydrophobic GDLs in this study. This exclusion, at this stage, aims to solely focus on the impact of patterned hydrophobic GDLs on the fuel cell performance and eliminate a layer of uncertainty by including the MPLs. However, for the interplay between MPL coating and the hydrophobic GDL pattern and its impact on the fuel cell performance is equally significant and warrants future investigation.

4. Conclusion

Flooding is a major issue in PEFCs and occurs when water generated at the cathode restricts the flow of oxygen from the gas channels through the GDL to the electrocatalyst. In this work, GDLs patterned with hydrophobicity gradient were fabricated to create distinct channels for water and oxygen transport, respectively. Three different patterns were formed simply by brushing the GDLs with a PTFE solution through a metal mask: (i) triangular; (ii) diamond-like; and (iii) inverted-triangular.

Surface treatment with 6-8% PTFE loading was sufficient to achieve the desired level of hydrophobicity without compromising porosity or conductivity – higher PTFE loadings resulted in no additional increase in contact angle.

Under fully humidified conditions and at a cell temperature of 80 °C, all the patterned GDLs successfully demonstrated improved fuel cell performance compared to uniformly treated GDLs, especially in the high current density region ($> 0.8 \text{ A/cm}^2$). Notably, the patterned GDLs also displayed lower oxygen transport resistance, confirming that the hydrophobicity gradient can aid water transport out of the electrocatalyst layer and mitigate flooding. As part of future work, we plan to systematically test the performance of the patterned GDLs under supersaturated conditions at low temperatures to assess their flooding mitigation capabilities in challenging operational environments.

Amongst the patterned GDLs, triangular patterning resulted in the best fuel cell performance. This was attributed to the fact that the less hydrophobic untreated region of the GDL was in contact with the cathode outlet, further facilitating removal of excess water from the cell. Overall, this work confirms that providing dedicated hydrophobicity gradient in the GDL for independent water and gas transfer via a simple masking technique can result in significant improvement in the fuel cell performance.

Our study on patterned hydrophobic GDLs for PEFCs demonstrates promising results with lower PTFE loading. While existing literature suggests an optimal PTFE content of around 20 wt. % for uniformly PTFE-treated GDLs (see, for example, [9] and [10]), this generalisation may not necessarily apply to patterned hydrophobic GDLs. Therefore, it will be of interest in the future to optimise the PTFE content for patterned hydrophobic GDLs.

Acknowledgements

The authors would like to thank the Daiwa Anglo Japanese Foundation (Ref: 13826/14659) for supporting the first author's research visit to Kyushu University. This work was also supported by JSPS KAKENHI Grant Number JP19H02558. The authors would like to thank Qizhi Ba and Rachel Smith's lab for help with the water contact angle measurement. The authors would also like to thank Havva Kiral for her help with the sketch of flow field with the patterned GDLs.

References

- [1] Falama RZ, Saidi AS, Soulouknga MH, Salah CB. A techno-economic comparative study of renewable energy systems based different storage devices. *Energy*. 2023 Mar 1;266:126411. <https://doi.org/10.1016/j.energy.2022.126411>
- [2] Calili-Cankir F, Ismail MS, Ingham DB, Hughes KJ, Ma L, Pourkashanian M. Air-breathing versus conventional polymer electrolyte fuel cells: A parametric numerical study. *Energy*. 2022 Jul 1;250:123827. <https://doi.org/10.1016/j.energy.2022.123827>
- [3] Hong, S., Kim, E. and Jeong, S., 2023. Evaluating the sustainability of the hydrogen economy using multi-criteria decision-making analysis in Korea. *Renewable Energy*, 204, pp.485-492. <https://doi.org/10.1016/j.renene.2023.01.037>
- [4] Calili-Cankir F, Ismail MS, Berber MR, Alrowaili ZA, Ingham DB, Hughes KJ, Ma L, Pourkashanian M. Dynamic models for air-breathing and conventional polymer electrolyte

fuel cells: A comparative study. *Renewable Energy*. 2022 Aug 1;195:1001-14.

<https://doi.org/10.1016/j.renene.2022.06.092>

[5] Daud WR, Rosli RE, Majlan EH, Hamid SA, Mohamed R, Husaini T. PEM fuel cell system control: A review. *Renewable Energy*. 2017 Dec 1;113:620-38.

<https://doi.org/10.1016/j.renene.2017.06.027>

[6] Calili F, Ismail MS, Ingham DB, Hughes KJ, Ma L, Pourkashanian M. A dynamic model of air-breathing polymer electrolyte fuel cell (PEFC): A parametric study. *International Journal of Hydrogen Energy*. 2021 May 13;46(33):17343-57.

<https://doi.org/10.1016/j.ijhydene.2021.02.133>

[7] Calili-Cankir F, Ismail MS, Ingham DB, Hughes KJ, Ma L, Pourkashanian M. Air-breathing polymer electrolyte fuel cells: A review. *Renewable Energy*. 2023 Jun 1.

<https://doi.org/10.1016/j.renene.2023.05.134>

[8] Lai T, Qu Z. Pore-scale parametric sensitivity analysis of liquid water transport in the gas diffusion layer of polymer electrolyte membrane fuel cell. *Applied Thermal Engineering*.

2023 Jul 5;229:120616. <https://doi.org/10.1016/j.applthermaleng.2023.120616>

[9] Giorgi L, Antolini E, Pozio A, Passalacqua E. Influence of the PTFE content in the diffusion layer of low-Pt loading electrodes for polymer electrolyte fuel cells. *Electrochimica Acta*. 1998 Aug 21;43(24):3675-80. [https://doi.org/10.1016/S0013-4686\(98\)00125-X](https://doi.org/10.1016/S0013-4686(98)00125-X)

[10] Velayutham G, Kaushik J, Rajalakshmi N, Dhathathreyan KS. Effect of PTFE content in gas diffusion media and microlayer on the performance of PEMFC tested under ambient pressure. *Fuel cells*. 2007 Aug;7(4):314-8. <https://doi.org/10.1002/fuce.200600032>

[11] Park GG, Sohn YJ, Yang TH, Yoon YG, Lee WY, Kim CS. Effect of PTFE contents in the gas diffusion media on the performance of PEMFC. *Journal of Power Sources*. 2004 May 14;131(1-2):182-7. <https://doi.org/10.1016/j.jpowsour.2003.12.037>

- [12] Ismail MS, Damjanovic T, Ingham DB, Ma L, Pourkashanian M. Effect of polytetrafluoroethylene-treatment and microporous layer-coating on the in-plane permeability of gas diffusion layers used in proton exchange membrane fuel cells. *Journal of Power Sources*. 2010 Oct 1;195(19):6619-28. <https://doi.org/10.1016/j.jpowsour.2010.04.036>
- [13] Ismail MS, Damjanovic T, Hughes K, Ingham DB, Ma L, Pourkashanian M, Rosli M. Through-plane permeability for untreated and PTFE-treated gas diffusion layers in proton exchange membrane fuel cells. <https://doi.org/10.1115/1.4000685>
- [14] Ismail MS, Damjanovic T, Ingham DB, Pourkashanian M, Westwood A. Effect of polytetrafluoroethylene-treatment and microporous layer-coating on the electrical conductivity of gas diffusion layers used in proton exchange membrane fuel cells. *Journal of Power Sources*. 2010;195(9):2700-8. <https://doi.org/10.1016/j.jpowsour.2009.11.069>
- [15] Alhazmi N, Ismail MS, Ingham DB, Hughes KJ, Ma L, Pourkashanian M. The in-plane thermal conductivity and the contact resistance of the components of the membrane electrode assembly in proton exchange membrane fuel cells. *Journal of Power Sources*. 2013;241:136-45. <https://doi.org/10.1016/j.jpowsour.2013.04.100>
- [16] Alhazmi N, Ingham DB, Ismail MS, Hughes K, Ma L, Pourkashanian M. The through-plane thermal conductivity and the contact resistance of the components of the membrane electrode assembly and gas diffusion layer in proton exchange membrane fuel cells. *Journal of Power Sources*. 2014;270:59-67. <https://doi.org/10.1016/j.jpowsour.2014.07.082>
- [17] Fishman, Z. and Bazylak, A., 2011. Heterogeneous through-plane porosity distributions for treated PEMFC GDLs I. PTFE effect. *Journal of The Electrochemical Society*, 158(8), p.B841. [DOI 10.1149/1.3594578](https://doi.org/10.1149/1.3594578)
- [18] Mortazavi M, Tajiri K. Effect of the PTFE content in the gas diffusion layer on water transport in polymer electrolyte fuel cells (PEFCs). *Journal of Power Sources*. 2014;245:236-44. <https://doi.org/10.1016/j.jpowsour.2013.06.138>

- [19] Gola M, Sansotera M, Navarrini W, Bianchi CL, Stampino PG, Latorrata S, Dotelli G. Perfluoropolyether-functionalized gas diffusion layers for proton exchange membrane fuel cells. *Journal of Power Sources*. 2014 Jul 15;258:351-5.
<https://doi.org/10.1016/j.jpowsour.2014.02.025>
- [20] Stampino PG, Latorrata S, Molina D, Turri S, Levi M, Dotelli G. Investigation of hydrophobic treatments with perfluoropolyether derivatives of gas diffusion layers by electrochemical impedance spectroscopy in PEM-FC. *Solid State Ionics*. 2012;216:100-4.
<https://doi.org/10.1016/j.ssi.2012.03.032>
- [21] Lim C, Wang CY. Effects of hydrophobic polymer content in GDL on power performance of a PEM fuel cell. *Electrochim Acta*. 2004;49(24):4149-56.
<https://doi.org/10.1016/j.electacta.2004.04.009>
- [22] Latorrata S, Stampino PG, Cristiani C, Dotelli G. Novel superhydrophobic microporous layers for enhanced performance and efficient water management in PEM fuel cells. *International Journal of Hydrogen Energy*. 2014;39(10):5350-7.
<https://doi.org/10.1016/j.ijhydene.2013.12.199>
- [23] Cabasso I, Yuan Y, Xu X, inventors; Research Foundation of State University of New York, assignee. Gas diffusion electrodes based on poly (vinylidene fluoride) carbon blends. United States patent US 5,783,325. 1998 Jul 21.
- [24] Lee FC, Ismail MS, Ingham DB, Hughes KJ, Ma L, Lyth SM, Pourkashanian M. Alternative architectures and materials for PEMFC gas diffusion layers: A review and outlook. *Renewable and Sustainable Energy Reviews*. 2022 Sep 1;166:112640.
<https://doi.org/10.1016/j.rser.2022.112640>
- [25] Can EM, Mufundirwa A, Wang P, Iwasaki S, Kitahara T, Nakajima H, et al. Superhydrophobic fluorinated carbon powders for improved water management in hydrogen

fuel cells. *Journal of Power Sources*. 2022;548.

<https://doi.org/10.1016/j.jpowsour.2022.232098>

[26] Can EM, Nishihara M, Matsuda J, Sasaki K, Lyth SM. Tailored wettability in fluorinated carbon nanoparticles synthesized from fluorotelomer alcohols. *Applied Surface Science*. 2023 Jul 30;626:157136. <https://doi.org/10.1016/j.apsusc.2023.157136>

[27] Forner-Cuenca A, Biesdorf J, Gubler L, Kristiansen PM, Schmidt TJ, Boillat P. Engineered water highways in fuel cells: radiation grafting of gas diffusion layers. *Advanced materials*. 2015 Nov;27(41):6317-22.

<https://doi.org/10.1002/adma.201503557>

[28] Forner-Cuenca A, Manzi-Orezzoli V, Biesdorf J, El Kazzi M, Streich D, Gubler L, et al. Advanced Water Management in PEFCs: Diffusion Layers with Patterned Wettability I. Synthetic Routes, Wettability Tuning and Thermal Stability. *Journal of The Electrochemical Society*. 2016;163(8):F788-F801. [DOI 10.1149/2.0271608jes](https://doi.org/10.1149/2.0271608jes)

[29] Forner-Cuenca A, Biesdorf J, Lamibrac A, Manzi-Orezzoli V, Buchi FN, Gubler L, et al. Advanced Water Management in PEFCs: Diffusion Layers with Patterned Wettability II. Measurement of Capillary Pressure Characteristic with Neutron and Synchrotron Imaging. *Journal of The Electrochemical Society*. 2016;163(9):F1038-F48. [DOI 10.1149/2.0511609jes](https://doi.org/10.1149/2.0511609jes)

[30] Forner-Cuenca A, Biesdorf J, Manzi-Orezzoli V, Gubler L, Schmidt TJ, Boillat P. Advanced Water Management in PEFCs: Diffusion Layers with Patterned Wettability. *Journal of The Electrochemical Society*. 2016;163(13):F1389-F98.

[DOI 10.1149/2.0891613jes](https://doi.org/10.1149/2.0891613jes)

[31] Manzi-Orezzoli V, Siegwart M, Cochet M, Schmidt TJ, Boillat P. Improved water management for PEFC with interdigitated flow fields using modified gas diffusion layers. *Journal of The Electrochemical Society*. 2019 Nov 26;167(5):054503.

[DOI 10.1149/2.0062005JES](https://doi.org/10.1149/2.0062005JES)

- [32] Torkaman R, Maleki F, Gholami M, Torab-Mostaedi M, Asadollahzadeh M. Assessing the radiation-induced graft polymeric adsorbents with emphasis on heavy metals removing: A systematic literature review. *Journal of Water Process Engineering*. 2021 Dec 1;44:102371. <https://doi.org/10.1016/j.jwpe.2021.102371>
- [33] Utaka Y, Hirose I, Tasaki Y. Characteristics of oxygen diffusivity and water distribution by X-ray radiography in microporous media in alternate porous layers of different wettability for moisture control in gas diffusion layer of PEFC. *International Journal of Hydrogen Energy*. 2011 Jul 1;36(15):9128-38. <https://doi.org/10.1016/j.ijhydene.2011.04.152>
- [34] Chun H, Kim Y, Chae H, Lee M, Han B, Kim M, Choi H, Hur JW, Kim HS, Ok JG. Facile airbrush fabrication of gas diffusion layers comprising fine-patterned hydrophobic double-layer and hydrophilic channel for improved water removal in polymer electrolyte membrane fuel cells. *International Journal of Precision Engineering and Manufacturing-Green Technology*. 2021 Sep;8:1461-9. <https://doi.org/10.1007/s40684-020-00254-y>
- [35] Zhang ZH, Guo MD, Yu ZH, Yao SY, Wang J, Qiu DK, et al. A novel cooperative design with optimized flow field on bipolar plates and hybrid wettability gas diffusion layer for proton exchange membrane unitized regenerative fuel cell. *Energy*. 2022;239. <https://doi.org/10.1016/j.energy.2021.122375>
- [36] Zhang W, Guo F, Zhou Y, Yu S, Chen A, Jiang H, Jiang H, Li C. Gas Diffusion Layer with a Regular Hydrophilic Structure Boosts the Power Density of Proton Exchange Membrane Fuel Cells via the Construction of Water Highways. *ACS Applied Materials & Interfaces*. 2022 Apr 6;14(15):17578-84. <https://doi.org/10.1021/acsami.2c03388>
- [37] Chen, L., Lin, R., Chen, X., Hao, Z., Diao, X., Froning, D. and Tang, S., 2020. Microporous layers with different decorative patterns for polymer electrolyte membrane fuel cells. *ACS applied materials & interfaces*, 12(21), pp.24048-24058. <https://doi.org/10.1021/acsami.0c05416>

- [38] Yu, J., Froning, D., Reimer, U. and Lehnert, W., 2019. Polytetrafluorethylene effects on liquid water flowing through the gas diffusion layer of polymer electrolyte membrane fuel cells. *Journal of power sources*, 438, p.226975.
<https://doi.org/10.1016/j.jpowsour.2019.22697>
- [39] Froning, D., Reimer, U. and Lehnert, W., 2021. Inhomogeneous distribution of polytetrafluorethylene in gas diffusion layers of polymer electrolyte fuel cells. *Transport in Porous Media*, 136, pp.843-862. <https://doi.org/10.1007/s11242-021-01542-0>
- [40] Koresawa R, Utaka Y. Improvement of oxygen diffusion characteristic in gas diffusion layer with planar-distributed wettability for polymer electrolyte fuel cell. *Journal of Power Sources*. 2014;271:16-24. <https://doi.org/10.1016/j.jpowsour.2014.05.151>
- [41] Smits FM. Measurement of sheet resistivities with the four-point probe. *Bell System Technical Journal*. 1958 May;37(3):711-8.
<https://doi.org/10.1002/j.1538-7305.1958.tb03883.x>
- [42] Barbir F. PEM Fuel Cells: Theory and Practice. Sustain World Ser. 2005:1-433.
- [43] Benziger J, Nehlsen J, Blackwell D, Brennan T, Itescu J. Water flow in the gas diffusion layer of PEM fuel cells. *Journal of membrane science*. 2005 Sep 15;261(1-2):98-106.
<https://doi.org/10.1016/j.memsci.2005.03.049>
- [44] Fairweather JD, Cheung P, Schwartz DT. The effects of wetproofing on the capillary properties of proton exchange membrane fuel cell gas diffusion layers. *Journal of Power Sources*. 2010;195(3):787-93. <https://doi.org/10.1016/j.jpowsour.2009.08.032>
- [45] Ismail MS, Ingham DB, Ma L, Pourkashanian M. The contact resistance between gas diffusion layers and bipolar plates as they are assembled in proton exchange membrane fuel cells. *Renew Energy*. 2013;52:40-5. <https://doi.org/10.1016/j.renene.2012.10.025>

[46] Mortazavi, M. and Tajiri, K., 2014. Liquid water breakthrough pressure through gas diffusion layer of proton exchange membrane fuel cell. *international journal of hydrogen energy*, 39(17), pp.9409-9419. <https://doi.org/10.1016/j.ijhydene.2014.03.238>

[47] Henning S, Adhikari R. Scanning Electron Microscopy, ESEM, and X-ray Microanalysis. *Micro Nano Technol.* 2017;1:1-30.